Hindawi Publishing Corporation
Chinese Journal of Engineering
Volume 2014, Article ID 658760, 5 pages
http://dx.doi.org/10.1155/2014/658760

Research Article

Time-Dependant Responses of High-Definition Induction Log and Case Studies

Jianhua Zhang and Zhenhua Liu

Science College, Xi'an Shiyou University, Xi'an 710065, China

Correspondence should be addressed to Jianhua Zhang; jhzhang@xsyu.edu.cn

Received 19 January 2014; Revised 27 April 2014; Accepted 4 May 2014; Published 19 May 2014

Academic Editor: Liang Li

The process of drilling mud filtrate invading into a reservoir is time dependant. It causes dynamic invasion profiles of formation parameters such as water saturation, salinity, and formation resistivity. Thus, the responses of a high-definition induction log (HDIL) tool are time dependent. The logging time should be considered as an important parameter during logging interpretation for the purposes of determining true formation resistivity, estimating initial water saturation, and evaluating a reservoir. The time-dependent HDIL responses are helpful for log analysts to understand the invasion process physically. Field examples were illustrated for the application of present method.

1. Introduction

Resistivity log is an effective method to estimate the critical properties of a reservoir in petroleum exploration. Induction log is an important tool to measure the formation resistivity. In addition to traditional dual-induction log tools [1], new array type induction devices [2], such as array induction tool (AIT) and high-definition induction log (HDIL), can provide more messages. The AIT device was designed with 10-, 20-, 30-, 60-, and 90-inch (25, 51, 76, 152, and 229 cm) depths of investigation, and the HDIL tool provides six depths of investigation, 10, 20, 30, 60, 90, and 120 inches (25, 51, 76, 152, 229, and 305 cm), respectively. The HDIL instrument is a typical multiarray induction logging tool that measures the formation resistivity simultaneously with six arrays.

However, the resistivity measurement is affected by invasion process strongly. When a reservoir was opened, drilling mud filtrate poured into permeable and porous formations; thus, an invaded zone was formed. The behaviors of the invaded zone are very different from the original formation. The physical understanding of an invasion process is essential for logging interpretation and reservoir evaluation. Conventional invasion model is the static step-invasion profile [3] that presumes that the resistivity varies sharply at the boundary between invaded zone and uncontaminated formation. In fact, the displacement of moveable native fluids in a reservoir by mud filtrate is a percolation process. The formation- and fluid-related parameters do not vary in a step-invasion style. In addition, a realistic invasion process is time dependant. At the beginning of bit penetration, the rate of invasion is rapid. With the lapse of time, mud cake is built at the wall of borehole. With the building of mud cake and the extension of invading geometry area, the invasion rate decreased.

The dynamic invasion process has a severe impact on logging tools. Logging at various time stages will lead to different measurement results, that is, time-dependant resistivity responses. The dynamic invasion process and its influences on resistivity-logging tools have been investigated internationally for traditional resistivity log tools [4–6] and new AIT devices [7, 8]. The present work focused on the influence of dynamic invasion process on HDIL measurements.

The theoretical model of dynamic invasion and the geometry factor theory for resistivity log were used to calculate the time-dependant responses of a HDIL device. The present results can give a reasonable interpretation for the difference of resistivity responses at various measurement times. In addition, comparing the dynamic model with static step-invasion style, the dynamic invasion profiles and time-dependant logging responses can provide more information

for log analysts to evaluate a reservoir and to understand the complexity of the invasion process.

The present model was used in a field located at west of China. Examples of field applications were illustrated to determine the true-formation resistivity and initial saturation and furthermore to evaluate a reservoir.

2. Dynamic Invasion Model

The time-dependent resistivity-logging model is based on dynamic invasion theory. During drilling, mud filtrate pours into the formation radially and displaces the native fluids in porous volumes under the pressure differential between borehole and formation. We supposed that the reservoir is thick and the displacement between filtrate and hydrocarbon is immiscible.

The invasion process is also related to formation parameters such as absolute permeability k, formation porosity φ, native-water salinity C_w, mud-filtrate salinity C_{mf}, relative permeability k_{ro} and relative permeability k_{rw}, original saturation S_o and original saturation S_w, formation pressure P_o and formation pressure P_w, fluid viscosity μ_w and fluid viscosity μ_o in formation, and fluid flow capacity q_o and fluid flow capacity q_w. We used subscript o for oil phase and w for water phase, respectively.

At the beginning of invasion, mud cake is built up promptly at the wall of borehole. With the extension of invading geometry area and the building of mud cake, the invasion rate slows down with time. The dynamic invasion process satisfied fluid flow equations [9] as in the following steps.

First, both saturation and pressure in reservoir are functions of invasion time t and radial distance r from the borehole. They can be solved from flow equations:

$$\begin{aligned} \frac{1}{r}\frac{\partial}{\partial r}\left(\frac{rkk_{ro}}{\mu_o}\frac{\partial P_o}{\partial r}\right) + q_o &= \frac{\partial(\varphi P_o S_o)}{\partial t}, \\ \frac{1}{r}\frac{\partial}{\partial r}\left(\frac{rkk_{rw}}{\mu_w}\frac{\partial P_w}{\partial r}\right) + q_w &= \frac{\partial(\varphi P_w S_w)}{\partial t}. \end{aligned} \tag{1}$$

In order to solve (1), the relationships $S_o + S_w = 1$ and $P_o - P_w = P_c$ were used. P_c is capillary pressure. It can be obtained from special core analysis.

Second, since the mud salinity C_{mf} is different from the salinity C_w of water in formation, the mixing of mud filtrate with native water causes the variation of salinity distribution with time during invasion process. The variation of water salinity is generated from the following dispersion equation after S_w and P_w were obtained from (1):

$$\frac{1}{r}\frac{\partial}{\partial r}\left(\frac{rkk_{rw}C_w}{\mu_w}\frac{\partial P_w}{\partial r}\right) + q_w C_{\mathrm{mf}} = \frac{\partial(\varphi S_w C_{\mathrm{mf}})}{\partial t}. \tag{2}$$

Third, the petrophysics formulas [4, 5] were used to generate the water resistivity R_w and formation resistivity R_f They are functions of both t and r. They can be determined from above-solved saturation and salinity.

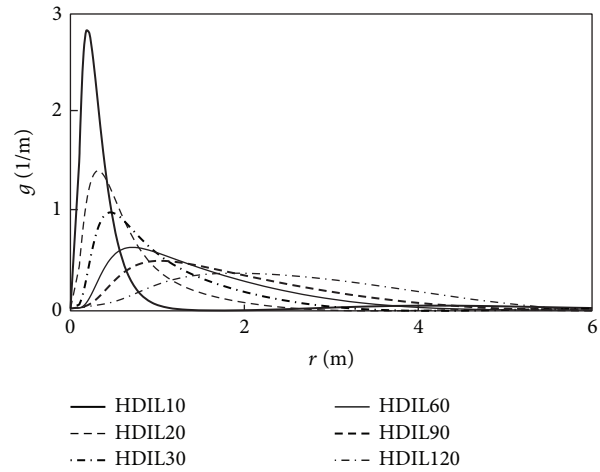

Figure 1: The radial differential geometrical factor for a HDIL device.

Consider

$$R_w = \left(0.0123 + \frac{3647.5}{C_w^{0.955}}\right)\cdot\frac{82}{39 + 1.8T}, \tag{3}$$

$$R_f = \frac{abR_w}{S_w^n \varphi^m}, \tag{4}$$

where T is the temperature (°C) in the reservoir, both a and b are constants, m is the cementation factor, and n is the saturation exponent.

3. Time-Dependent Responses of HDIL Devices

Since the radial distribution of formation resistivity varies with time, the apparent resistivity of HDIL measurement at time t is determined by resistivity invasion profile $R_f(t, r)$. According to the theory of geometry factor for induction log [1], the apparent resistivity R_a of a HDIL device is

$$R_a(t) = \left[\int_0^\infty \frac{g(r)}{R_f(t, r)}dr\right]^{-1}, \tag{5}$$

where $g(r)$ is radial differential geometrical factor.

The apparent resistivity readings of a HDIL device, R_a, vary with measurement time t. The variation is the physical basis of time-dependant HDIL measurement.

A HDIL device is composed of seven three-coil arrays at 8 operating frequencies (10, 30, 50, 70, 90, 110, 130, and 150 kHz, resp.) [2]. It provides six apparent resistivities, which are usually marked as HDIL10, HDIL20, HDIL30, HDIL60, HDIL90, and HDIL120. They correspond to six detective depths: 10, 20, 30, 60, 90, and 120 inches (25, 51, 76, 152, 229, and 305 cm), respectively.

Figure 1 illustrated the radial differential geometrical factor g for each array of a HDIL device. The region of g peak makes the greatest contribution to apparent resistivity according to (5). Therefore, the HDIL10 array is influenced by

the vicinity of borehole strongly and has the shallowest detective depth. The HDIL120 array has maximum investigation depth; hence, it can reflect the character of resistivity far away from the borehole. The detective depth of a HDIL device will increase according to the arrays HDIL10, HDIL20, HDIL30, HDIL60, HDIL90, and HDIL120, as shown in Figure 1.

4. Time-Dependant HDIL Measurements and Their Applications

The present model of dynamic invasion effects on time-dependant HDIL measurement was applied in a reservoir located at west of China.

4.1. An Oil-Bearing Reservoir. The bed was logged at 25 days after the formation was opened. The field logging data for HDIL10, HDIL20, HDIL30, HDIL60, HDIL90, and HDIL120 were 10.0, 10.5, 12.7, 18.5, 22.0, and 28.0 ohm·m, respectively.

History-matching method [4, 5] was used to simulate the time-dependant responses of HDIL measurement. The simulation began with an initial estimation of water saturation S_w. In order to reach the best matching with well logging data, the initial water saturation was set to be 0.32 for the present field example. The other main necessary input data were $C_w = 40000$ mg/L, $C_{\mathrm{mf}} = 26700$ mg/L, $\varphi = 0.055$, $k = 0.001\,\mu\mathrm{m}^2$, $\mu_w = 0.4$ cp, $\mu_o = 0.452$ cp, $T = 110^\circ$C, $m = 1.65$, $n = 1.57$, $a = 0.89$, and $b = 1.05$ in (4). The pressures of borehole and original reservoir were 70 MPa and 65 Mpa, respectively.

Figures 2 and 3 showed the present calculation for radial profiles of water saturation S_w from (1) and water salinity C_w from (2), respectively. The horizontal axis denoted the distance from borehole. Since the diameter of borehole in present simulation was 8 inches, the radial invasion curves were drawn from the wall of borehole.

Since the well was filled with mud during drilling, the water saturation in borehole was high. In Figure 2, the line marked with $t = 0$ means the initial water saturation before invasion occurs ; it corresponds to the value of S_w, 0.32. At the beginning of mud invasion, the well was filled with mud filtrate. After the formation was opened, the filtrate began to pour into the reservoir, so that the water saturation was high at the adjacency of borehole. Figure 2 showed the radial invasion profiles of water saturation at 4, 10, 23, and 50 days, respectively, after the mud filtrate poured into the formation.

In the present case study, the initial water salinity C_w was 40000 mg/L, which was greater than mud salinity of 26700 mg/L, so that the salinity profile near the wellbore was low. With the lapse of time, the low-salinity filtrate invaded into the reservoir so that the radial profile of water salinity changed, as shown in Figure 3.

The changes of both saturation and salinity lead to the alternations of water resistivity and formation resistivity. According to (3), the water resistivity was determined by water salinity. The low-salinity fresh filtrate near the borehole leads to the high water resistivity, as shown in Figure 4. With the lapse of time, this high water-resistivity profile moved into the deeper formation.

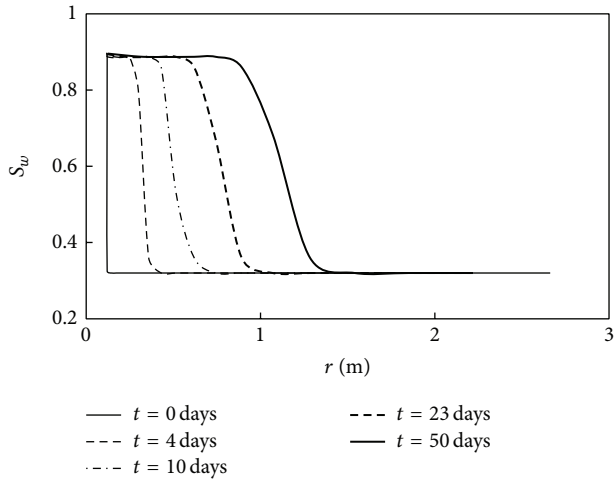

Figure 2: Radial invasion profiles of water saturation.

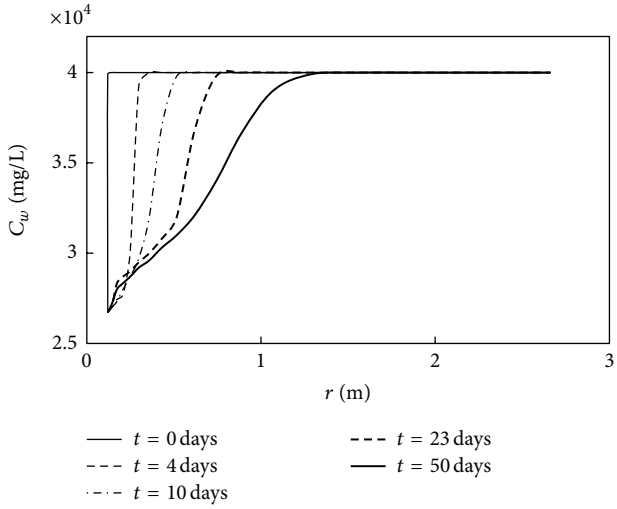

Figure 3: Radial invasion profiles of water salinity.

Formation resistivity R_f was obtained from (4). It was determined both by time-dependant water saturation S_w and by water resistivity R_w. Hence, the profiles of formation resistivity changed with time as well. They were drawn in Figure 5 for four time stages, 4, 10, 23, and 50 days, in the invasion process.

High water saturation and high water resistivity in the vicinity of borehole caused a low-resistivity range, in which the physical characters were very different from the original formation. After 20 days of the mud invading, the invasion depth reached one meter (Figure 5). The resistivity distribution in formation does not vary sharply at the boundary between the invaded zone and noninvaded area.

The change of R_f with time leads to the time-dependant responses of the HDIL measurement. The lines in Figure 6 illustrated the calculation results of various HDIL readings with time using (5). The horizontal axis denoted the logging time after the formation was immersed and the vertical axis

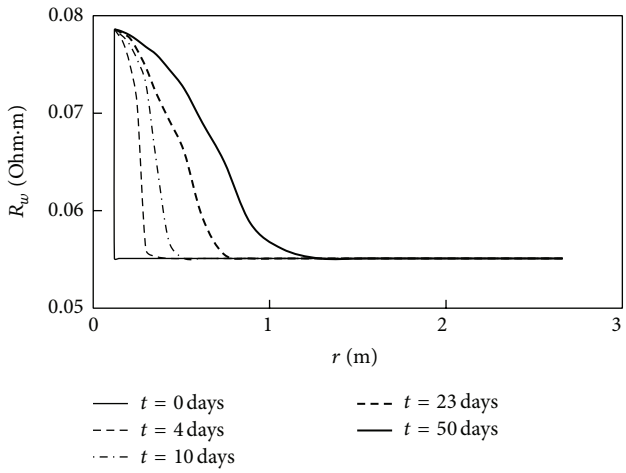

Figure 4: Radial invasion profiles of water resistivity.

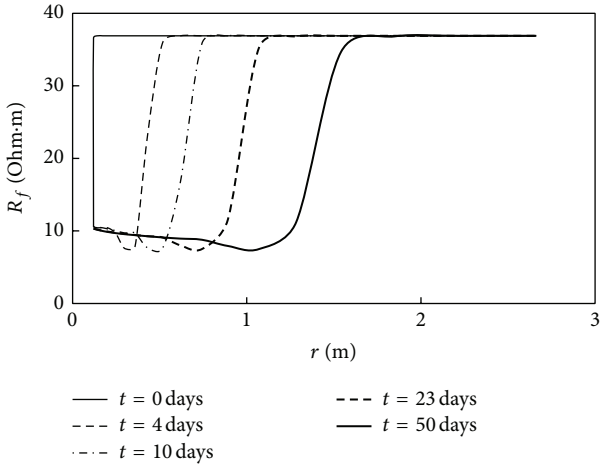

Figure 5: Radial invasion profiles of formation resistivity.

was the apparent resistivity of HDIL measurement. The dots in Figure 6 were the logging data.

After the formation was opened, the invasion zone moved into the reservoir gradually. When the low-resistivity invasion zone in Figure 5 reached the detective depth of the HDIL array, the logging readings decreased according to (5). Since HDIL10 has the shallowest detective depth and HDIL120 has the deepest investigation depth, the HDIL10 array reached its minimum value and HDIL120 array got its maximum reading. For the present field example, the result, HDIL120 > HDIL90 > HDIL60 > HDIL30 > HDIL20 > HDIL10, was obtained.

The present simulation suggested the true-formation resistivity R_t is equal to 36.9 ohm·m, which just corresponded to the value before invasion occurrence, that is, the apparent resistivity at $t = 0$ in Figure 6. It also reflected the initial water saturation setting, $S_w = 0.32$, according to (4). The low value of initial water saturation illustrated the behaviors of an oil-bearing reservoir with high oil saturation, $S_o = 1 - S_w = 0.68$, for the present field application.

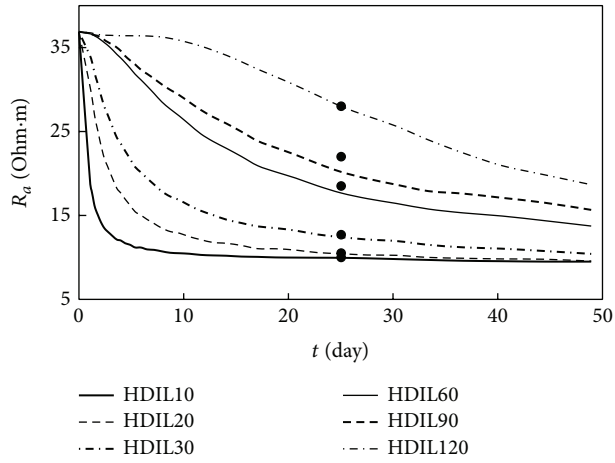

Figure 6: Time-dependent HDIL responses for an oil-bearing reservoir (lines were the results of present simulation and the dots were the logging data).

For this case application, all of the field HDIL readings were less than the true resistivity, because of the influence of low-resistivity invasion zone, as shown in Figure 5. Therefore, if the logging data were used to estimate the true-formation resistivity directly, error would be introduced. The calculation results of history-matching were also helpful for log analysts to understand the characters of dynamic invasion process physically.

4.2. A Water Zone. A water-bearing formation shows different characters. Figure 7 illustrated a simulation result of field example for a water zone. This bed was located in the same well, with the reservoir simulated in Figures 2~6. The measurement results for HDIL10, HDIL20, HDIL30, HDIL60, HDIL90, and HDIL120 were 3.52, 3.30, 3.25, 3.18, 3.17, and 3.19 ohm·m, respectively, after the formation was invaded for 30 days.

During the history-matching, the main input data were the same as in Figures 2~6 for the same well. The time-dependant HDIL responses were illustrated using lines and the logging data were marked by dots, respectively, in Figure 7.

The present simulation suggested that the initial water saturation S_w was equal to 0.8, and the true-formation resistivity R_t was 3.26 ohm·m, which corresponded to the apparent resistivity at $t = 0$ in Figure 7, that is, before invasion occurrence. The present history-matching suggested the reservoir was a water zone with high water saturation, 0.8.

If a reservoir is filled by movable water, it has high water saturation. When native saline water with low resistivity was replaced by fresh mud filtrate with high resistivity, a high-resistivity invasion zone formed near to the borehole. It influenced the responses of shallow detective HDIL arrays much more, so that the apparent resistivities of shallow detective arrays were usually greater than the values measured from the arrays of deeper investigation depths after the formation was immersed for a long time period, as shown in Figure 7.

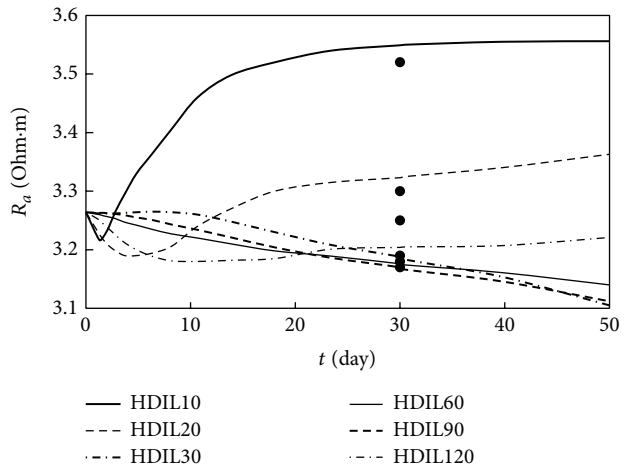

Figure 7: Time-dependent HDIL responses for a water bed (lines were the results of present simulation and the dots were the logging data).

5. Conclusions

There is not a sharp boundary between invaded zone and uncontaminated formation. The invasion profiles of formation parameters, such as water saturation, salinity, and resistivity, show complex shapes. It is important that the process of drilling mud filtrate invading into a reservoir is time related, so that the invasion profiles vary with time as well. This dynamic invasion style is very different from the traditional static step-invasion model.

The profiles of formation parameters vary with time. It leads to that the apparent resistivities from the measurement of a high-definition induction log device are time-dependant . The different logging data measured at various time stages will cause confused log interpretations, so that errors or incorrect evaluation would be introduced.

The logging time is suggested to be recorded as a parameter in order to get a reasonable interpretation for HDIL measurements. The time-dependant apparent resistivities of a HDIL device can be obtained using the dynamic invasion model and resistivity-logging theory.

The history-matching method can be used to obtain the true-formation resistivity and initial fluid saturation in a reservoir from the present simulation of time-dependant HDIL measurement. Site applications in a well located at west of China proved the validity of the present method in log interpretation and reservoir evaluation.

Time-dependant log is a useful technique in geophysical exploration. It has successful applications such as rock physics model describing [10] and cross-hole electrical resistivity tomography monitoring [11].

Conflict of Interests

The authors declare that there is no conflict of interests regarding the publication of this paper.

References

[1] J. Tittman, *Geophysical Well Logging*, Academic Press, Orlando, Fla, USA, 1986.

[2] M. Gonfalini and M. T. Galli, "Array Induction measurements in complex environments: a comparison between AIT and HDIL responses," in *Proceedings of the SPE Annual Technical Conference and Exhibition*, pp. 3451–3466, Society of Petroleum Engineers, New Orleans, La, USA, October 2001.

[3] E. Head, D. Allen, and L. Colsdon, "Quantitative invasion description," in *Proceedings of the 33rd Annual Logging Symposium*, pp. B1–B21, Society of Petrophysicists and Well-Log Analysts, Oklahoma City, Okla, USA, 1992.

[4] C. Y. Yao and S. A. Holditch, "Reservoir permeability estimation from time-lapse log data," *SPE Formation Evaluation*, vol. 11, no. 2, pp. 69–74, 1996.

[5] J. H. Zhang, Q. Hu, and Z. H. Liu, "Estimation of true formation resistivity and water saturation with a time-lapse induction logging method," *The Log Analyst*, vol. 40, no. 2, pp. 38–148, 1999.

[6] J. M. Sun, S. Y. Zheng, and J. H. Ma, "A new method for connate water saturation calculation using time-lapse logging data," *Journal of Petroleum Science and Engineering*, vol. 50, no. 3-4, pp. 204–210, 2006.

[7] Y. R. Fan, H. Li, Y. Y. Hu, and Q. T. Sun, "Numerical simulation of array induction logs time-lapse responses and formation resistivity profile reconstruction with 5-parameter inversion," *Advanced Materials Research*, vol. 588-589, pp. 1359–1363, 2012.

[8] J. H. Liu, Z. H. Liu, and J. H. Zhang, "Computation of time-dependent AIT responses for various reservoirs using dynamic invasion model," in *Recent Advances in Computer Science and Information Engineering*, vol. 125 of *Lecture Notes in Electrical Engineering*, pp. 823–828, Springer, Berlin, Germany, 2012.

[9] G. W. Thomas, *Principles of Hydrocarbon Reservoir Simulation*, International Human Resources Development Corporation, Boston, Mass, USA, 1982.

[10] N. Takahiro and Z. Q. Xue, "Evaluation of of a resistivity model derived from time-lapse well logging of a pilot-scale CO_2 injection site, Nagaoka, Japan," *International Journal of Greenhouse Gas Control*, vol. 12, pp. 288–299, 2013.

[11] F. Bellmunt, A. Marcuello, J. Ledo et al., "Time-lapse cross-hole electrical resistivity tomography monitoring effects of an urban tunnel," *Journal of Applied Geophysics*, vol. 87, pp. 60–70, 2012.